DOI: 10.1002/ejic.200800617

Synthesis, Structural, Magnetic and Thermal Characterization of $\{[Cu(bipy)]_2(\mu\text{-}HP_2O_7)(\mu\text{-}Cl)\}\cdot H_2O$

Oluwatayo F. Ikotun,[a] Elizabeth M. Higbee,[a] Wayne Ouellette,[a] Francesc Lloret,[b] Miguel Julve,*[b] and Robert P. Doyle*[a]

Keywords: Copper complexes / Pyrophosphate / Polynuclear compounds / Magnetic coupling

Copper(II) hydroxide reacts with 2,2′-bipyridine (bipy) and sodium pyrophosphate in a 2:2:1 stoichiometric ratio under ambient conditions at pH 1.6 in water. The resulting neutral dinuclear Cu^{II} complex features a bridging set containing bridging monoprotonated pyrophosphate and a monoatomic chloro bridge (making this the first pyrophosphate bridged coordination complex containing an alternate, additional halide bridge between the metal centers). Single-crystal X-ray diffraction studies revealed the complex to be $\{[Cu(bipy)]_2(\mu\text{-}HP_2O_7)(\mu\text{-}Cl)\}\cdot H_2O$. The structure consists of a dimeric copper(II) system with each metal ion in a square pyramidal geometry. The asymmetric $[Cu(bipy)]^{2+}$ units are bridged by bis-bidentate pyrophosphate and an axially bridging chlorine atom. The incorporation of an additional bridge (halide) and the presence of protonated pyrophosphate ($HP_2O_7^{3-}$) in the structure are both rare for this family of structures. Intermolecular π–π interactions between the bipy ligands from adjacent dinuclear complexes and hydrogen bonding between the lattice water molecule and the bridging chloro atom create a 1D network. Variable-temperature magnetic susceptibility measurements show the occurrence of a weak antiferromagnetic interaction with a maximum at 3.0 K. The analysis of the magnetic data in the whole temperature range (1.9–300 K) allows the determination of the value of the intramolecular magnetic coupling ($J = -3.19\ cm^{-1}$, the Hamiltonian being defined as $\hat{H} = -J\hat{S}_A \cdot \hat{S}_B$). This value of J is significantly lower than that observed for the analogous dicopper(II) system devoid of the bridging chloro group. Reasons for this difference and its importance are discussed.

Introduction

The pyrophosphate tetra-anion was first characterized almost two hundred years ago[1] and it has since drawn considerable interest in the fields of ceramic, electrical, magnetic, and catalytic applications.[2] The multidentate nature of pyrophosphate makes it an attractive ligand for the formation of multinuclear complexes with varied structural types and properties. With the small but increasing library of structurally characterized pyrophosphate-based coordination complexes,[3] it remains imperative to investigate the structural and functional diversity of the ligand and evolve it beyond discrete complexes and/or integrate additional bridges into such complexes.

One of the first and integral reports in the field involved the pyrophosphate-bridged dicopper(II) complex, $\{[Cu(bipy)(H_2O)]_2(\mu\text{-}P_2O_7)\}\cdot 7H_2O$,[4] (bipy = 2,2′-bipyridine), which spurred us to investigate the possibility of affecting the magnetic exchange by incorporation of additional bridges alongside the bridging pyrophosphate. This dicopper(II) species underwent a ca. 5.5 fold increase in the strength of the antiferromagnetic coupling upon dehydration giving a coupling constant of $J = -110\ cm^{-1}$. We postulated that an additional exchange pathway was formed between alternate layers, and reasoned a new monoatomic (μ-oxo) bridge was forming. Since that time we have been endeavoring to synthesize a "model" of that predicted structure with an additional monoatomic bridge to investigate the structure and magneto-functional effects in depth. Such a structure would also open up the possibility of generating a new series of compounds whereby a variety of additional bridges could be incorporated. This would offer the possibility of conducting an in-depth structure-magneto functional correlation for a whole new class of pyrophosphate-bridged complexes. We report herein the synthesis, characterization, thermal and magnetic properties of a discrete pyrophosphate coordination complex containing an additional (μ-Cl) bridging group between the metal centers (see Figure 1). This structure contains monoprotonated bridging pyrophosphate, something rarely observed in the reported structures to date[3f] Comparison is made (based on the negligible magnetic contribution of the bridging

[a] Department of Chemistry, Syracuse University, Syracuse, NY 13244-4100, USA
Fax: +1-315-443-4070
E-mail: rpdoyle@syr.edu
[b] Departament of Química Inorgànica/Instituto de Ciencia Molecular (ICMol) Universitat de València, Polígono la Coma s/n, 46980 Paterna, València, Spain
E-mail: miguel.julve@uv.es

Supporting information for this article is available on the WWW under http://www.eurjic.org or from the author.

chloro group) in terms of magnetic properties (given the significant structural impact of the additional bridge), between the original dicopper(II) complex (see Figure 2) and the new structure described herein (see Figure 1).

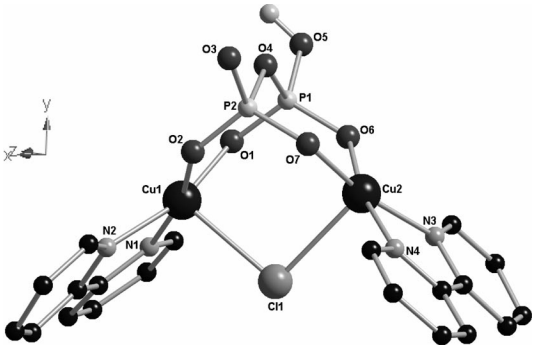

Figure 1. ORTEP plot of **1** with the atomic-labeling scheme. Hydrogen atoms and the water of crystallization have been removed for clarity. Note the presence of a hydroxy group (O5) on the hydrogenpyrophosphate ligand.

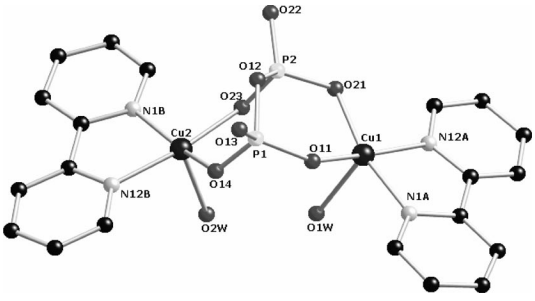

Figure 2. Molecular structure of $\{[(bipy)Cu(H_2O)]_2(\mu\text{-}P_2O_7)\cdot 7H_2O\}$ (**2**) with atom numbering. Hydrogen atoms and the water molecules of crystallization have been omitted for clarity.

Results and Discussion

Synthesis and Characterization of $\{[Cu(bipy)]_2(\mu\text{-}HP_2O_7)(\mu\text{-}Cl)\}\cdot H_2O$ (1)

An aqueous suspension of copper(II) hydroxide was brought into solution by decreasing the pH to 1.6 with 6 M hydrochloric acid. An aqueous suspension of 2,2′-bipyridine was added in 1:1 Cu^{II}–bipy molar ratio to the acidified solution, and a sky-blue solution resulted upon stirring. The addition of a 0.5 stoichiometric equivalence of solid sodium pyrophosphate was followed by the formation over several minutes of a blue solid, which was re-dissolved in water by increasing the pH to ca. 8.5 with 1 M NaOH. Blue parallelepipeds of **1** were grown by slow evaporation at room temperature over 30 d. The infrared spectrum of this product indicated the presence of pyrophosphate with P–O–P stretches observed at 1194, 1113, and 1057 cm^{-1}. The bipy bands were observed at 1446 and 772 cm^{-1}.[5] Electrospray mass spectrometry gave peaks at m/z = 544.70 and 554.75, which were assigned to the solvated species, $\{[Cu_2(bipy)(\mu\text{-}HP_2O_7)(\mu\text{-}Cl)(H_2O)(MeOH)] + H^+\}$ and $\{[Cu_2(bipy)(\mu\text{-}HP_2O_7)(\mu\text{-}Cl)(H_2O)(MeCN)] + H^+\}$ respectively (with loss of bipy occurring in situ). The electronic absorption spectrum exhibited a broad featureless band centered at 662 nm, which is consistent with the presence of a Cu^{II} chromophore with distorted square-pyramidal geometry.[6] It was also noted that green crystals were formed alongside the blue crystals. These blocks were determined to be $\{[Cu(bipy)Cl]_2(\mu\text{-}Cl_2)]\}$ via X-ray diffraction studies.[7]

Crystal Structure of 1

Compound **1** crystallizes in the monoclinic $P2_1/n$ space group. The molecular structure of **1** consists of neutral $\{[Cu(bipy)]_2(\mu\text{-}HP_2O_7)(\mu\text{-}Cl)\}$ dinuclear copper(II) units with two crystallographically unique copper atoms, Cu(1) and Cu(2). The molecular structure with the atomic labeling Scheme is shown in Figure 1.

Each copper(II) ion is in a distorted square pyramidal geometry. The basal plane consists of the N_2O_2 coordination chromophore, which is derived from two nitrogen atoms from the bipy ligand and two oxygen atoms from the bridging hydrogenpyrophosphate. The square pyramidal geometry is completed with a bridging chloro group occupying the axial position of the copper(II) ion. Similar to previously reported pyrophosphato-bridged homodinuclear Ni^{II}, Mn^{II}, Co^{II}, and Cu^{II} complexes,[4,8,9] the hydrogenpyrophosphate group coordinates to the metal center in a bisbidentate coordination mode, forming a six-membered chelate ring at each copper atom. The copper(II) ions are shifted from the N_2O_2 basal plane toward the bridging chloro group by 0.234 [Cu(1)] and 0.185 Å [Cu(2)].

The copper–copper distance in **1** is 3.954 Å, a significantly smaller distance compared to that observed in the previously reported pyrophosphate-bridged dicopper(II) complex **2** (intradimer distance of 4.646 Å).[4] The shortest interdimer Cu···Cu distance in **1** is 8.649 Å. Key bond lengths and angles are shown in Table 1.

Table 1. Selected bond lengths [Å] and angles [°] for **1**.

Cu(1)–O(2)	1.9461(10)	O(2)–Cu(1)–O(1)	95.48(4)
Cu(1)–O(1)	1.9560(11)	O(2)–Cu(1)–N(2)	90.41(5)
Cu(1)–N(2)	2.0064(13)	N(2)–Cu(1)–N(1)	80.21(5)
Cu(1)–N(1)	2.0089(12)	O(1)–Cu(1)–Cl(1)	95.80(3)
Cu(1)–Cl(1)	2.6267(5)	N(1)–Cu(1)–Cl(1)	95.70(4)
Cu(2)–O(7)	1.9459(11)	O(1)–Cu(1)–N(2)	161.09(5)
Cu(2)–O(6)	1.9516(11)	N(3)–Cu(2)–N(4)	80.37(5)
Cu(2)–N(3)	1.9997(13)	O(7)–Cu(2)–O(6)	96.31(4)
Cu(2)–N(4)	2.0042(13)	N(3)–Cu(2)–Cl(1)	94.98(4)
Cu(2)–Cl(1)	2.6581(5)	O(6)–Cu(2)–Cl(1)	95.55(3)
P(1)–O(6)	1.5115(11)	O(6)–Cu(2)–N(3)	90.05(5)
P(1)–O(1)	1.5138(11)	O(7)–Cu(2)–N(4)	91.34(5)
P(1)–O(5)	1.5325(11)	Cu(1)–Cl(1)–Cu(2)	96.86(4)
P(1)–O(4)	1.6065(10)	O(6)–P(1)–O(1)	115.03(6)
P(2)–O(3)	1.5097(11)	O(2)–P(2)–O(7)	113.46(6)
P(2)–O(4)	1.6264(10)	P(1)–O(4)–P(2)	121.11(7)

The dihedral angle between the two mean equatorial planes of **1** is 83.67°, a value which is sharply acute in contrast with that of **2** (132.8°). The additional bridge has

caused a dramatic change of 49.3° between these two structures. The presence of the chloro-bridge doubtless incorporated as a consequence of pyrophosphate protonation results in other subtle changes in the structure of **1** when compared to that of **2**. The tetrahedral environment of the phosphorus atom in **1** has been slightly altered to accommodate the chloro-bridge (see Table 2). The protonation itself is illustrated by the different P–O bond lengths, [P(1)–O(5)] of 1.532 Å in **1**, longer than the comparable bond [P(1)–O(13)] 1.498 Å in **2**, which is consistent with the switch from double- to single-bond character (the H atoms were also located in a difference map and refined freely in the X-ray single crystal structural studies). Complex **1** is a rare example of a protonated bridging pyrophosphato motif.

Table 2. Selected bond lengths [Å] and angles [°] around the phosphorus atom of the pyrophosphate groups in **1** and **2**.[4]

1		**2**	
Bond lengths			
P(1)–O(1)	1.5138(11)	P(1)–O(11)	1.527(4)
P(1)–O(4)	1.6065(10)	P(1)–O(12)	1.632(4)
P(1)–O(5)	1.5325(11)	P(1)–O(13)	1.496(4)
P(1)–O(6)	1.5115(11)	P(1)–O(14)	1.526(4)
P(2)–O(2)	1.5176(11)	P(2)–O(21)	1.521(4)
P(2)–O(3)	1.5097(11)	P(2)–O(22)	1.496(4)
P(2)–O(4)	1.6065(10)	P(2)–O(12)	1.615(4)
P(2)–O(7)	1.5228(11)	P(2)–O(23)	1.534(4)
Bond angles			
O(1)–P(1)–O(6)	115.03(6)	O(11)–P(1)–O(14)	112.6(2)
O(4)–P(1)–O(5)	104.70(6)	O(12)–P(1)–O(13)	105.0(2)
O(4)–P(1)–O(1)	107.67(6)	O(12)–P(1)–O(11)	106.4(2)
O(4)–P(1)–O(6)	107.26(6)	O(12)–P(1)–O(14)	106.3(2)
O(5)–P(1)–O(1)	111.55(6)	O(13)–P(1)–O(11)	112.8(2)
O(5)–P(1)–O(6)	109.99(6)	O(13)–P(1)–O(14)	113.0(2)
O(2)–P(2)–O(7)	113.46(6)	O(21)–P(2)–O(23)	110.8(2)
O(4)–P(2)–O(2)	106.23(6)	O(12)–P(2)–O(21)	107.5(2)
O(4)–P(2)–O(7)	106.12(6)	O(12)–P(2)–O(23)	105.1(2)
O(4)–P(2)–O(3)	105.03(6)	O(12)–P(2)–O(22)	106.2(2)
O(3)–P(2)–O(2)	113.62(6)	O(22)–P(2)–O(21)	112.7(2)
O(3)–P(2)–O(7)	111.56(6)	O(22)–P(2)–O(23)	113.9(2)

Average carbon–carbon and carbon–nitrogen bond lengths are close to those reported for the free bipyridine molecule.[10] Similar to **2**, the bipy ligands interact via intermolecular face-edge π-π interactions with a separation at closest contact of 4.0 Å.

Additionally, the system's packing is facilitated by intermolecular hydrogen bonding between the lattice water and the chloro ligand [Cl···O(90) = 3.238 Å; 1/2 – *x*, – 1/2 + *y*, 1.5 – *z*] and between protonated O(5) of a pyrophosphate moiety and O(3) of an adjacent dimer [(O(3)··· H(5′) = 1.543 Å; 1/2 – *x*, –1/2 + *y*, 1.5 – *z*, see Figure 3 and Figure S3 (Supporting Information)]. There is no solvent access volume in **1**, in contrast to complex **2**, with a solvent occupancy of ca. 17% (which contrasts strongly with the dinickel(II) complex $\{[Ni(phen)_2]_2(\mu\text{-}P_2O_7)\}\cdot 27H_2O$,[8] which has the highest solvent occupancy at 45.7%). This is reflected in the greater density of **1** (1.959 g cm^{-3}) compared to those of **2** (1.720 g cm^3) and the dinickel(II) species (1.485 g cm^{-3}).

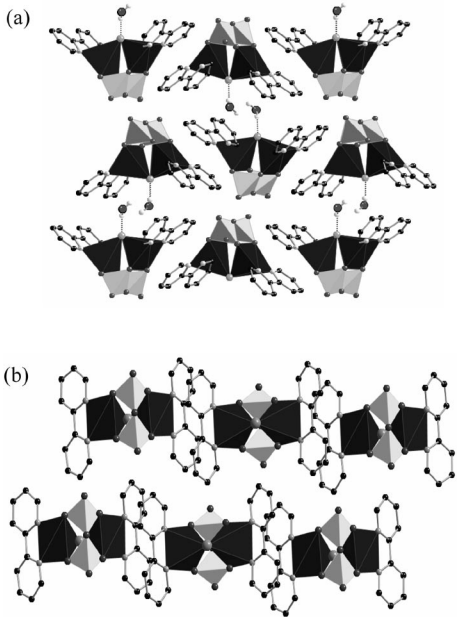

Figure 3. (a) Packing diagram of **1** down the crystallographic *a*-axis showing the intermolecular H-bonding mediated by the lattice water and bridged chloro ligand. (b) Packing diagram down the *b* crystallographic axis showing the intermolecular π-π interactions in **1**. Lattice water and hydrogen atoms are omitted for clarity.

Thermal Analysis of 1

Thermogravimetric analysis (TGA) was performed on a powdered sample of the compound to primarily investigate the degree of solvation of the complex. The sample was ramped from ca. 25 to 500 °C at a rate of 10 °C/min under a dinitrogen atmosphere. The TGA curve of **1** is shown in Figure 4. The slight inflection at ca. 50 °C after a mass loss of 15.32% is indicative of the loss of seven water molecules. When samples of the compound were vacuum dried overnight, the trace was calculated, by elemental analysis and TGA, to contain one water molecule. Decomposition of the dinuclear species at ca. 150 °C is consistent with the loss of a bipy ligand.

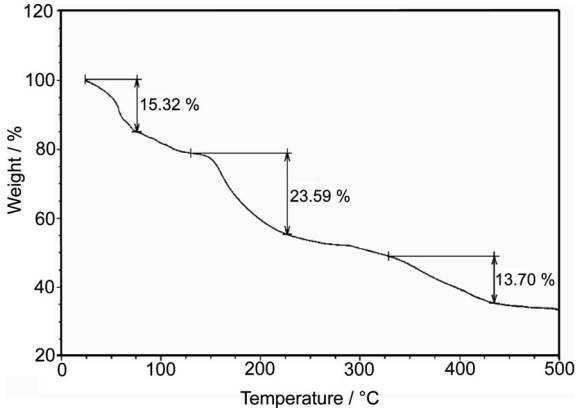

Figure 4. TGA curve of **1** indicating the loss of solvent and the subsequent decomposition of the dinuclear species at ca. 150 °C.

Magnetic Behaviour of 1

The magnetic properties of complex **1** (as the crystalline monohydrate) in the form of both $\chi_M T$ and χ_M vs. T (χ_M is the magnetic susceptibility per two copper(II) ions) are shown in Figure 5. At room temperature, $\chi_M T$ is equal to 0.84 $cm^3 mol^{-1} K$, a value which is expected for two magnetically isolated copper(II) ions. This value remains constant upon cooling to 30 K and then it decreases sharply to ca. 0.26 $cm^3 mol^{-1} K$ at 1.9 K. The susceptibility vs. T plot (see inset of Figure 5) exhibits a maximum at 3.0 K. These features are characteristic of the occurrence a weak intramolecular antiferromagnetic interaction.

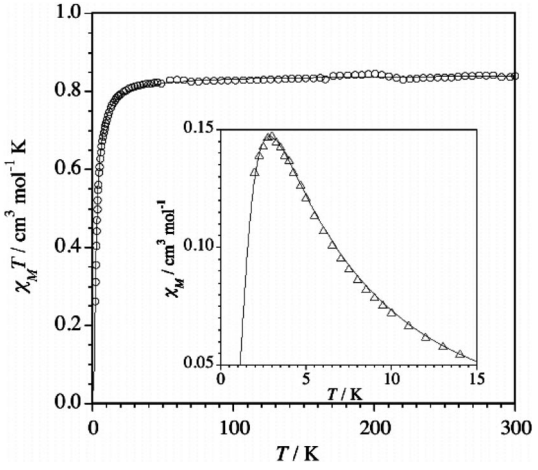

Figure 5. Thermal dependence of the ($\chi_M T$) product for **1**: (o) experimental data; (—) best-fit curve through Equation (1) (see text). The inset shows the (χ_M) vs. (T) plot in the vicinity of the maximum.

Keeping in mind the dinuclear structure of **1**, we have analyzed the magnetic data by a simple Bleaney–Bowers law for two interacting spin doublets [Equation (1)].

$$\chi_M = 2N\beta^2 g^2/kT\,[3 + \exp(-J/kT)]^{-1} \quad (1)$$

which is derived through the Hamiltonian $\hat{H} = -J\hat{S}_A \cdot \hat{S}_B$ where J is the magnetic coupling, g is the average Landé factor and N, β, k and T have theirs usual meanings. Best-fit parameters through Equation (1) are $J = -3.19\ cm^{-1}$, $g = 2.12$ and $R = 5 \times 10^{-5}$ {R is the agreement factor defined as $\Sigma[(\chi_M)_{obsd} - (\chi_M)_{calcd}]^2/\Sigma[(\chi_M)_{obsd}]^2$}. As shown in Figure 5, the calculated curve matches the experimental data very well through the whole temperature range.

Relevant magneto-structural data on pyrophosphato-bridged complexes with first-row transition metal ions are listed in Table 3. In all these examples, the pyrophosphate ligand adopts the bis-bidentate coordination mode and the magnetic coupling is relatively weak and antiferromagnetic in nature. As previously discussed, the magnetic interaction along a family of homometallic dinuclear complexes with different sidzes of interacting local spins is not properly described by J, but by $n_A n_B J$.[9,11] Given that the energy of the 3d orbitals decreases when moving from Mn^{II} to Cu^{II}, the energy gap between these orbitals (the so-called magnetic orbitals when describing unpaired electrons) and of the symmetry-adapted HOMOs of the bridging hydrogenpyrophosphate becomes smaller when going from left to right in a row of the periodic Table. This would cause a better overlap between the magnetic orbitals when going from Mn^{II} to Cu^{II} thus increasing the antiferromagnetic interaction along this series (Table 3).

However, complex **1** exhibits a much weaker antiferromagnetic coupling than its parent dicopper(II) complex {[(bipy)Cu(H_2O)]$_2$(μ-P_2O_7)·7H_2O} (**2**). Complex **2**, upon dehydration, had a J value of –110 cm^{-1}. It is clear that the presence of the bridging chloro in **1** (occupying the apical position of the copper(II) ions) contributes significantly to the reduction of the antiferromagnetic coupling through the pyrophosphate bridge. This additional bridge causes a significant reduction of the intramolecular metal–metal separation (3.954 Å in **1** vs. 4.646 Å in **2**) and a further distortion of the Cu(1)-pyrophoshato–Cu(2) skeleton. The acuteness in **1** accounts for the observed weakening of the antiferromagnetic coupling. The unpaired electron on each copper(II) ion in **1** and **2** is described by a ($d_{x^2-y^2}$) type magnetic orbital (the x and y axes being roughly defined by the short Cu–N equatorial bonds). Because of the long axial Cu–Cl bond in **1** (ca. 2.6 Å), the spin density on the apical chloro atom is predicted to be very small. Weak magnetic couplings between copper(II) ions through single chloro-bridged copper(II) complexes where the equatorial-axial pathway is involved have been well documented.[12] Consequently, given that in **1** this pathway is of axial-axial type, one can safely conclude that the Cu(1)–Cl(1)–Cu(2) exchange pathway is negligible.[12] As the two magnetic orbitals are closer to coplanarity in **2**, the predicted overlap between them is stronger than that observed in **1**. The stronger the overlap between the magnetic orbitals, the larger the antiferromagnetic interactions are predicted to be. In the near future, theoretical calculations will be performed to analyze the

Table 3. Selected magneto-structural data for pyrophosphato-bridged dinuclear metal complexes.

Compound	M–O(pyro)[a] [Å]	d_{M-M}[b] [Å]	$-J$[c] [cm^{-1}]	n_A–$n_B J$[d] [cm^{-1}]	Ref.
{[Ni(phen)$_2$]$_2$(μ-P_2O_7)}·27H_2O	2.057	5.031	3.8	15.2	[8]
{[Mn(phen)$_2$]$_2$(μ-P_2O_7)}·13H_2O	2.105	4.700	0.88	22.0	[8]
{[Co(phen)$_2$]$_2$(μ-P_2O_7)}·6MeOH	2.043	4.857	1.23	11.1	[9]
{[Cu(bipy)(H_2O)]$_2$(μ-P_2O_7)}·7H_2O	1.950	4.646	20	20	[4]
{[Cu(bipy)]$_2$(μ-HP_2O_7)(μ-Cl)}·H_2O	1.950	3.954	3.19	3.19	this work

[a] Average value for the *meta*-oxygen (bridging pyrophosphate ligand) bond. [b] Metal–metal distance across the pyrophosphato-bridge. [c] Magnetic coupling through the pyrophosphate ligand. [d] n_A and n_B are the number of the unpaired electrons on the metal atoms A and B of the dinuclear AB complex.

role of this dihedral angle on the magnetic coupling in pyrophosphato-bridged dicopper(II) complexes once a broad array of such complexes becomes available.

Conclusions

We have successfully synthesized a protonated pyrophosphate ($HP_2O_7^{3-}$)-bridged discrete coordination complex incorporating a bridging chloro group. While recent interest in pyrophosphate complexes has provided us with several new structures, several targets remain in this field including synthesizing pyrophosphate complexes with increasingly complex dimensionality and/or producing mixed metal pyrophosphate bridged species. In addition, pyrophosphate complexes that incorporate additional bridging systems have not been reported until this work. The presence of this additional bridge has resulted in significant structural changes when **1** is compared to that of a previously reported non-chloro bridged analogue with increased acuteness of equatorial planes around the metal center and decreased metal–metal distance noted. These structural variations significantly affect the overall magnetic coupling observed in this compound as was hoped when the structure was first hypothesized. In fact, the inclusion of the chloro-bridge has significantly diminished the antiferromagnetic coupling through the pyrophosphato-bridge when compared to the non-chloro bridged analogue. In the previously reported structure, $\{[(bipy)Cu(H_2O)]_2(\mu\text{-}P_2O_7)\}\cdot 7H_2O$[4] (**2**), the magnetic coupling ($J = -20\ cm^{-1}$) is ca. sixfold smaller in comparison to that of **1** ($J = -3.19\ cm^{-1}$). The substantial change in the magnetic coupling can be attributed to the weakened overlap between the magnetic orbitals (d_{x-y}), resulting in weaker antiferromagnetic interactions. The reported complex **1** is critical in our attempt to better understand the magneto-structural correlation in pyrophosphate-bridged species, allowing us to understand the contribution of the dihedral angle, for example. Furthermore, we feel this structure will open the field to a whole new series of pyrophosphate structures with alternate bridges (e.g. bromo, flouro, perchlorate, etc.), especially given the facile nature of chloro incorporation demonstrated herein. We look forward to seeing the diverse structures and functions these new complexes may impart. Such new complexes would be an excellent arena for theoretical investigations of structure-magneto-functional relationships. This work is currently underway in our group.

Experimental Section

General: Solvents and chemicals were of laboratory grade and were used as received. Electrospray mass spectrometry was performed on a Shimadzu LCMS-2010 A system at a cone voltage of 5 kV. Infrared spectra were recorded on a Nicolet Magna-IR 850 Series II spectrophotometer as KBR pellets. Thermal analysis was performed on a TA instruments TGA Q500 using 1–6 mg samples placed on platinum pans and ran under a nitrogen atomosphere (40 mL/min). The temperature was ramped from ca. 25 to 500 °C at a rate of 10 °C/min. Analysis was performed using the TA instruments Universal Analysis 2000 software program. Elemental analysis (C, H, N) was performed by Intertek, Whitehouse, NJ. Water was distilled and deionized to 18.6 MΩ using a Branstead Diamond RO Reverse Osmosis machine coupled to a Branstead Nano Diamond ultrapurification machine. Centrifugation was carried out on a Sorvall RT machine at 4000 rpm for 10 min at room temperature. Variable-temperature magnetic susceptibility measurements were performed on a Quantum design SQUID susceptometer in the temperature range 1.9–300 K with an applied magnetic field $H = 1000$ G. Crystalline samples were obtained directly from the reaction mixture, air-dried and powdered in a mortar. Diamagnetic corrections for the constituent atoms were estimated using Pascal's constants and corrections for the sample holder and the temperature independent paramagnetism were also performed. Electronic absorption spectra were obtained on a Varian Cary 50 Bio spectrophotometer in 1-mL quartz cuvettes between 200 nm and 400 nm at ambient temperature.

Synthesis of $\{[Cu(bipy)]_2(\mu\text{-}HP_2O_7)(\mu\text{-}Cl)\}\cdot H_2O$: Copper(II) hydroxide (0.05 g, 0.51 mmol) was dissolved in 15 mL of water, and was brought into solution with the addition of 6 N hydrochloric acid to a pH of 1.6. To this was added an aqueous suspension of 2,2-bipyridine (0.079 g, 0.51 mmol) resulting in an aqua bluish solution. Solid sodium pyrophosphate (0.069 g, 0.26 mmol) was added directly and a blue precipitate was observed over several minutes. The precipitate was collected by centrifugation and resuspended in water. The pH was slowly increased with 1 M NaOH and a blue solution was obtained at a pH of 8.5. This solution was allowed to stand over ca. one month to give dark blue parallelepipeds which were suitable for X-ray structural studies. $C_{20}H_{21}ClCu_2N_4O_9P_2$ (667.86): calcd. C 35.02, H 3.09, N 8.17; found C 35.36, H 3.47, N 7.90. λ_{max}/nm: 662. FTIR (KBr): $\tilde{\nu}$ = 3448 (br), 1446 (m), 1194 (s), 1113 (s), 1057 (s), 1110 (m), 772 (m), 731 (w), 618 (m), 562 (w) cm^{-1}. ESMS (MeH): $[Cu(bipy)Cl]^+$ 255.18 $[Cu_2(bipy)(\mu\text{-}HP_2O_7)(\mu\text{-}Cl)(H_2O)(MeOH) + H]^+$ 544.70, $[Cu_2(bipy)(\mu\text{-}HP_2O_7)(\mu\text{-}Cl)(H_2O)(MeCN) + H]^+$ 554.75 *m*/*z*. Yield 9% based on Cu^{II}.

Structure Determination and Refinement: Structural measurements were performed on a Bruker-AXS SMART-CCD diffractometer at low temperature (90 K) using graphite-monochroated Mo-K_α radiation ($\lambda = 0.71073$ Å). Absorption corrections were applied using SADABS[13] and SHELXTL[14] The H atoms were located in a dif-

Table 4. Crystallographic details for **1**.

Chemical formula	$C_{20}H_{19}ClCu_2N_4O_8P_2$
Formula weight	667.86
Crystal system	monoclinic
Space group	$P2_1/n$
λ (Mo-K_α) [mm^{-1}]	0.71073
a [Å]	8.5083(12)
b [Å]	15.582(2)
c [Å]	17.177(2)
α [°]	90
β [°]	96.158(2)
γ [°]	90
V [$Å^3$]	2264.1(6)
Z	4
D_c [$g\,cm^{-3}$]	1.959
θ_{max} [°]	28.27
R, *wR*2 [$I > 2\sigma(I)$]	0.0215, 0.0566
R, *wR*2 (all data)	0.0223, 0.0571
Reflections	
collected	23462
observed	5606

ference map and refined freely. The structures were solved by direct methods and refined using the SHELXTL program package. Key crystallographic data is given in Table 4.

CCDC-690085 contains the supplementary crystallographic data for **1**. These data can be obtained free of charge from The Cambridge Crystallographic Data Centre via www.ccdc.cam.ac.uk/data_request/cif.

Supporting Information (see also the footnote on the first page of this article): Figure S1 shows the dihedral angle changes in **1** vs. **2** and Figure S2 shows the intermolecular H-bonding in **1**.

Acknowledgments

We thank the Alliance of Graduate Education and the Professoriate Program (AGEP) for a fellowship for OFI, the iLEARN program for funding for EMB, Syracuse University, and the Ministerio Español de Ciencia y Tecnología (Project CTQ2007–61690) for funding.

[1] E. J. Griffith, R. L. Buxton, *J. Am. Chem. Soc.* **1967**, *89*, 2884–2890.
[2] a) T. Kasuga, M. Terada, M. Nogamin, M. Niinomi, *J. Mater. Res.* **2001**, *16*, 876–880; b) S. T. Wilson, B. M. Lok, C. A. Messian, T. R. Cannon, E. M. Flanigen, *J. Am. Chem. Soc.* **1982**, *104*, 1146–1147; c) J. M. Thomas, *Angew. Chem. Int. Ed. Engl.* **1994**, *33*, 963–989; d) X. Sun, X. G. Xu, Y. J. Fu, S. L. Wang, H. Zeng, Y. P. Li, *Cryst. Res. Technol.* **2001**, *36*, 465–470.
[3] a) R. P. Doyle, M. Nieuwenhuyzen, P. E. Kruger, *Dalton Trans.* **2005**, *23*, 3745; b) J. Y. Xu, J. L. Tian, Q. W. Zhang, J. Zhao, S. P. Yan, D. Z. Liao, *Inorg. Chem. Commun.* **2008**, *11*, 69–72; c) Y. Funahashi, A. Yoneda, C. Taki, M. Kosuge, T. Ozawa, K. Jitsukawa, H. Masuda, *Chem. Lett.* **2005**, *34*, 1332–1333; d) X.-Y. Yi, Q.-F. Zhang, T. C. H. Lam, E. Y. Y. Chan, I. D. Williams, W.-H. Leung, *Inorg. Chem.* **2006**, *45*, 328–335; e) C. du Peloux, P. Mialane, A. Dolbecq, J. Marrot, F. Secheresse, *Angew. Chem. Int. Ed.* **2002**, *41*, 2808–2810; f) J. L. Kissick, A. M. Chippindale, *Acta Crystallogr., Sect. E: Struct. Rep. Online* **2002**, 58, m80; g) A. M. Chippindale, *Chem. Mater.* **2000**, *12*, 818–822.
[4] P. E. Kruger, R. P. Doyle, M. Julve, F. Lloret, M. Nieuwenhuyzen, *Inorg. Chem.* **2001**, *40*, 1726–1727.
[5] K. Nakamoto in *Infrared and Raman Spectra of Inorganic and Coordination Compounds*, Part B (Applications in Coordination, Organometallics and Bioinorganics), 5th ed., Wiley, Chichester, **1997**.
[6] F. A. Cotton, G. Wilkinson, *Advanced Inorganic Chemistry*, 5th ed., Wiley, New York, **1999**.
[7] G. E. Kostakis, E. Nordlander, M. Haukka, J. C. Plakatouras, *Acta Crystallogr., Sect. E: Struct. Rep. Online* **2006**, *62*, 77.
[8] O. F. Ikotun, N. G. Armatus, M. Julve, P. E. Kruger, F. Lloret, M. Nieuwenhuyzen, R. P. Doyle, *Inorg. Chem.* **2007**, *46*, 6668–6674.
[9] O. F. Ikotun, W. Ouellette, F. Lloret, P. E. Kruger, M. Julve, R. P. Doyle, *Eur. J. Inorg. Chem.* **2008**, 2691–2697.
[10] L. L. Merrit, E. D. Schroeder, *Acta Crystallogr.* **1956**, *9*, 801–804.
[11] O. Kahn, *Struct. Bonding (Berlin, Ger.)* **1987**, *68*, 89–167 and references cited therein.
[12] H. Grove, J. Sletten, M. Julve, F. Lloret, *J. Chem. Soc., Dalton Trans.* **2001**, 2487–2493 and references cited therein.
[13] Bruker, SADABS, Software Reference Manual, Bruker AXS Inc. Madison, Wisconsin, USA, **2000**.
[14] G. M. Sheldrick, *SHELXTL PC*, version 6.1; Bruker-AXS Inc.: Madison, WI, **2000**.

Received: June 17, 2008
Published Online: October 16, 2008

